Extreme Mechanics Letters 65 (2023) 102107

Contents lists available at ScienceDirect

Extreme Mechanics Letters

journal homepage: www.elsevier.com/locate/eml

Elucidating the hydrogen influence on twin nucleation in FeNiCr medium-entropy alloy

Jinjin Guo [a], Shuozhi Xu [b], Dengke Chen [a,*]

[a] Department of Engineering Mechanics, School of Naval Architecture, Ocean and Civil Engineering, Shanghai Jiao Tong University, Shanghai 200240, China
[b] School of Aerospace and Mechanical Engineering, University of Oklahoma, Norman, OK 73019, USA

ARTICLE INFO

Keywords:
Hydrogen embrittlement
Medium-entropy alloys
Twinning
Molecular dynamics

ABSTRACT

This study employs atomistic simulations to investigate the intricate interplay between hydrogen and twinning nucleation in FeNiCr medium entropy alloys (MEA). The observed effects of hydrogen on nucleation reveal a dualistic nature. Homogeneous twinning nucleation adheres to the classic Pascal distribution, facilitated by hydrogen, while surface-bound hydrogen inhibits this process. These findings underscore the intricate interplay between hydrogen and twinning mechanisms, emphasizing the distinct effects of internal and surface-bound hydrogen. The presence of twin architecture significantly enhances the alloy's overall strength, ductility, and toughness. This study's multifaceted analysis of hydrogen's influence on twinning nucleation adds complexity to understanding hydrogen's broader impact on MEA mechanical properties. The profound comprehension of the hydrogen-twinning relationship contributes to addressing hydrogen embrittlement concerns, offering insights for material design and durability enhancement.

1. Introduction

The potential of the hydrogen economy holds both promise and challenge, spanning various dimensions including hydrogen generation, transportation, and storage [1]. One critical concern in the application of hydrogen to metals is its impact on mechanical performance, commonly referred to as hydrogen embrittlement (HE) [2–7]. Conventional alloying techniques typically revolve around a single primary element, whereas high/medium-entropy alloys (HEAs/MEAs) take a distinct approach by incorporating multiple principal elements at equiatomic or near-equatomic ratios, resulting in complex solid solutions with exceptional strength and ductility [8–15]. Notably, some HEAs/MEAs exhibit marginal decreases in ductility, fatigue strength, and fracture resistance when exposed to gaseous hydrogen [16–19].

The presence of twin architecture significantly contributes to the alloy's overall strength, ductility, and toughness; thus, many researchers focus on the hydrogen role in the nanotwinned structure. Soundararajan et al. [20] delved into the impact of hydrogen on deformation behavior and microstructure evolution in an MEA. Their investigation, employing electron channeling contrast images near cracks, revealed a notable density of nanotwins, indicating hydrogen's potential enhancement of twinning. Furthermore, Li et al. [21] documented that hydrogen could potentially decrease stacking fault energy (SFE), thereby promoting twinning. The presence of hydrogen was found to augment the alloy's load stress through an initial-strengthening effect, thereby influencing twinning occurrence. Luo et al. [22] conducted in-situ tensile tests and observed that the strength and ductility of CoCrFeMnNi increased with rising twinning density due to heightened hydrogen concentration.

It is crucial to recognize that existing understanding concerning hydrogen-twinning relationship in HEAs and MEAs primarily stem from experimental investigation. Nevertheless, prevailing experimental conditions often lack effective control over hydrogen distribution. This highlights the imperative of atomic simulation endeavors to elucidate the impacts of varied hydrogen distributions on the twinning process. Thus, in this letter, we plan to attain a profound comprehension of hydrogen role in the twinning nucleation in FeNiCr MEA through a comprehensive exploration of the hydrogen-twinning relationship. The structure of the paper unfolds as follows. **Section 2** presents atomic simulations of FeNiCrH systems, scrutinizing the influence of hydrogen on homogeneous twinning nucleation. In Section 3, atomic simulations are conducted to explore the hydrogen role in occurrence and behavior of surface twinning, in which the total hydrogen are situated on the simulation surface. In Section 4, surface twinning is revisited with a particular emphasis on examining the role of equilibrium hydrogen

* Corresponding author.
E-mail address: dengke.chen@sjtu.edu.cn (D. Chen).

https://doi.org/10.1016/j.eml.2023.102107
Received 5 September 2023; Received in revised form 20 October 2023; Accepted 20 November 2023
Available online 22 November 2023

atmosphere. Finally, Section 5 summarizes our study's pivotal discoveries and offers suggestions for prospective research directions.

2. Atomistic modeling of twinning nucleation

2.1. Simulation setup

To explore the effect of hydrogen atoms on the twinning nucleation, we have conducted molecular dynamics (MD) simulations to study the twinning process in equiatomic FeNiCr and FeNiCrH systems respectively. Fig. 1 presents the detailed atomistic configuration of the simulation setup for FeNiCr MEA. The simulation cell has dimensions of $7 \times 19 \times 6\text{nm}^3$ and contains a total number of ~58,000 atoms in which the Fe, Ni and Cr elements are randomly distributed. The periodic boundary conditions were imposed in the $X-[11\bar{2}]$ and $Z-[1\bar{1}0]$ directions, while the surfaces along the $Y-[111]$ directions were maintained traction-free. Two 1.5-nm-thick slabs were fixed at the top and bottom surfaces of the simulation cell. The shear load was applied by imposing a displacement-controlled boundary condition on the top slab, while the bottom slab remained fixed.

The simulations were carried out using the LAMMPS [23] atomistic simulation package, employing an embedded atom method potential specifically developed by Zhou et al. [24] for the FeNiCrH system. The visualization tool OVITO [25] was utilized to perform the common neighbor analysis to clearly display the stacking faults and nanotwin boundaries. During the simulation, the applied shear strain $\gamma_{xy} = 0.04$ was gradually exerted and then fixed in the canonical ensemble (NVT) at finite temperature $T = 600$K. MD simulation allowed for the observation and recording of the twinning nucleation process, facilitating subsequent analysis and investigation. In the FeNiCrH system, hydrogen atoms were randomly inserted into octahedral sites within the simulation cell. To quantitatively assess the hydrogen concentration, the hydrogen fraction parameter was introduced to represent the ratio of total hydrogen atoms to all metallic atoms. It has been noted that varying the strain rate at finite temperature can have a more or less significant impact on the mechanical behavior of materials [26–28]. To prevent such issues, we have chosen a method involving a substantial number of cycles with small displacements at 0 K. In each cycle, energy minimization is achieved using the conjugate gradient method. Strain loading precedes the use of the NVT ensemble, and the strain value is then maintained until twinning occurs. This approach helps ensure consistent and controlled conditions in our simulations.

2.2. Statistical distribution of twinning nucleation

Traditional twinning theory insists that the deformation twin in face-centered cubic (FCC) metals is achieved through layer-by-layer movement of partial dislocations on close-packed atomic planes [29]. Previous literature has proposed that the time required for dislocation nucleation follows the Poisson distribution [30]. However, according to the probability theory and statistics, the Pascal distribution with success number $r = 1$ might be better probability model than that of Poisson distribution [31]. Thus, we assume the time required for twinning nucleation follows the Pascal distribution.

To be specific, the total MD simulation time t_{total} is discretized into n time intervals (or called steps), in which the duration time of each interval is $\Delta t = t_{\text{total}}/n$. Imagine a sequence of independent interval: each interval has two potential outcomes called "twinning nucleation occurs" or "twinning nucleation fails". In each interval the probability of twinning nucleation is p and of failure is $1 - p$. Then the total random number of intervals k corresponding to the observation of the first twinning nucleation follows the Pascal distribution. And the probability mass function is

$$f(k,p) = (1-p)^{k-1} \bullet p \tag{1}$$

If we consider the variable $\nu_t = (k \bullet \Delta t)^{-1}$ as the elementary twinning nucleation rate, then the theoretical mean nucleation rate can be defined as

$$\langle \nu_t \rangle = \sum_{k=1}^{n} \nu_t \bullet f(k,p) \approx \frac{p\ln(1/p)}{(1-p)\Delta t} \tag{2}$$

Here, we consider the parameter metric of nucleation rate $\langle \nu_t \rangle$ to quantitatively assess the difficulty level of the twinning nucleation.

We have conducted MD simulations with20 independent samples for each hydrogen fraction (e.g., the total hydrogen fraction $\chi_0 = 0.0001$), where each simulation spanned a total time of $t_{\text{total}} = 1000$ps. Employing a duration time $\Delta t = 100$ps, we divided the total time into $n = t_{\text{total}}/\Delta t = 10$ intervals. For the kth interval, i.e., the time $t = k \bullet \Delta t$, we analyzed the unnucleated twinning ratio $u(k,p)$, i.e., the ratio of samples without observing twinning process across the total 20 samples. This yields the simulated unnucleated ratio as a function of the time interval. Drawing on above-mentioned probability theory, the theoretical

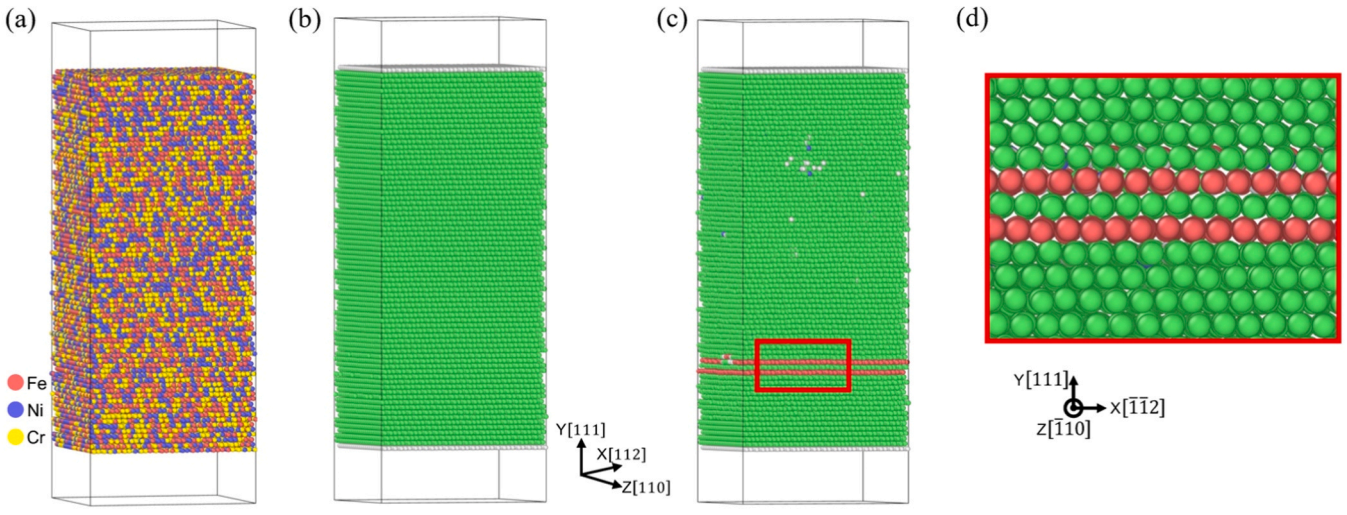

Fig. 1. Atomistic simulation of FeNiCr twinning process. (a) Simulation setup of random FeNiCr MEA. (b) Initial and (c) twinning atomic configurations of simulation cell. (d) Side view of magnified image of the boxed region in (c), showing the twinning configuration. Here the atomic structure visualization tool OVITO is used for common neighbor analysis, so as to identify atoms with hexagonal-close packed (HCP) structure (red), atoms with face-centered cubic (FCC) structure (green), and atoms on the surface (gray).

unnucleated ratio at the kth interval $u(k,p)$ is defined as

$$u(k,p) = (1-p)^k \tag{3}$$

The appropriate choice of Δt depends on both the shear strain and temperature. Specifically, at higher shear strain rates and elevated temperatures, twinning nucleation becomes more likely. Therefore, in these conditions, it is advisable to select a smaller Δt for recording the twinning nucleation process. Conversely, when dealing with low strain rates and lower temperature, a larger Δt can be chosen. It's worth noting that the probability parameter p is directly linked to Δt and exhibits a monotonically increasing trend as Δt is increasing. After we choose the appropriate Δt, we can capture the probability value p through curve fitting and obtain the mean nucleation rate of $\langle \nu_t \rangle$.

2.3. Simulation results: homogeneous twinning nucleation

Fig. 2 illustrates simulation outcomes concerning twinning nucleation process across various hydrogen fractions for FeNiCrH system. Evidently, the unnucleated ratio satisfies the anticipated power-law stated in Eq. (3). This verifies the application of Pascal distribution in characterizing the time required for homogeneous twinning nucleation in the FeNiCr MEA. Through curve fitting, we derive a twinning nucleation probability of $p = 0.26$. Additionally, Fig. 2b displays the calculated mean twinning nucleation rate $\langle \nu_t \rangle$ based on the established twinning probability according to Eq. (2). As the hydrogen fraction increases, the mean twinning nucleation rate also rises, implying that hydrogen atoms facilitate the homogeneous twinning nucleation. This observation aligns with the experimental findings of prior studies [17,18], which highlight the enhanced twinning nucleation attributed to hydrogen in MEAs.

Fig. 2c-e present detailed atomistic configurations of twinning nucleation process. It reveals that twin nucleation in FeNiCrH system is accomplished through the formation of twinning partial dislocations on consecutive atomic planes, i.e., the layer-by-layer stacking fault [29]. Thus, the observed hydrogen-enhanced twinning might be attributed to the hydrogen-enhanced nucleation of partial dislocation, which has been thoroughly investigated in the literatures. For example, Wen and Li [32] revealed that the hydrogen atoms lower the activation energy and thereby enhance homogeneous dislocation nucleation (HDN) in FCC Ni. Zhou et al. [33] observed the similar phenomenon of hydrogen-enhanced HDN in FCC Ni and Pd, but attributed this to the hydrogen-induced local expansion. The former emphasizes on the chemical effect of hydrogen on HDN, and the latter focuses on the mechanical effect. For the FeNiCrH system, chemical and mechanical effects may be both working in the HDN and the following twinning nucleation process. Furthermore, due to the intrinsic chemical disorders in MEA/HEA, even in the random solid solution state, a certain level of chemical heterogeneity/fluctuation at the atomic level is inevitable. This leads to a spatially distributed local stacking fault energy [34–36]. Hydrogen's interaction with this chemical heterogeneity and hydrogen effect on the stacking fault energy may also play a crucial role in the twinning nucleation process, which will be investigated in future work.

3. Atomistic modeling of surface twinning nucleation

As we have known, in comparison to being located within the bulk octahedrons, hydrogen atoms tend to locate on the surface of the material as well [5]. This section focuses on understanding how this surface-based localization of hydrogen atoms affects the process of twinning nucleation in the FeNiCrH system. To facilitate the investigation, we have modified the simulation setup to incorporate three traction-free boundaries, intentionally placing all hydrogen atoms on the surfaces.

As shown in Fig. 3a, the relationship between the unnucleated ratio and the time interval does not satisfy the theoretically predicted exponential form, i.e., $(1-p)^k$, for any fixed hydrogen fraction. Consequently, the applicability of the proposed mean twinning ratio is limited in scenarios involving free boundaries. However, it is evident that higher hydrogen fractions lead to an increase in the unnucleated ratio, thereby impeding the twinning nucleation. This observation contrasts with the

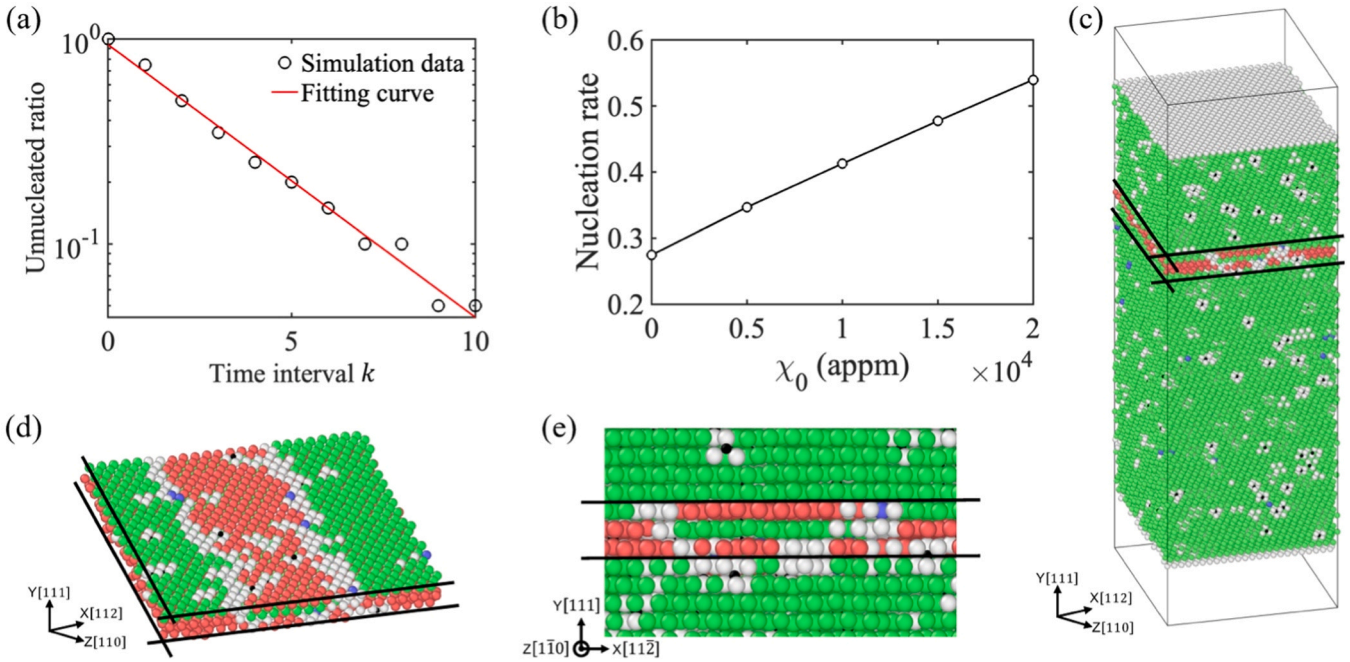

Fig. 2. MD simulation results of twinning nucleation in FeNiCr and FeNiCrH systems. (a) Unnucleated twinning ratio $u(k,p)$ versus time interval k in the logarithmic scale at a shear strain $\gamma_{xy} = 0.04$ and a temperature $T = 600$K. (b) Mean twinning nucleation rate $\langle \nu_t \rangle$ as a function of hydrogen fractions χ_0 for FeNiCrH system. (c) Perspective view of twinning nucleation process in random FeNiCrH system, in which hydrogen atoms are denoted by black spheres. (d) Magnified view of the denoted region in (c), revealing detailed snapshot of twinning nucleation. (e) Magnified side view of the denoted region in (c). In (c)-(e), the black lines serve as guides to show nanotwinned structure in different views.

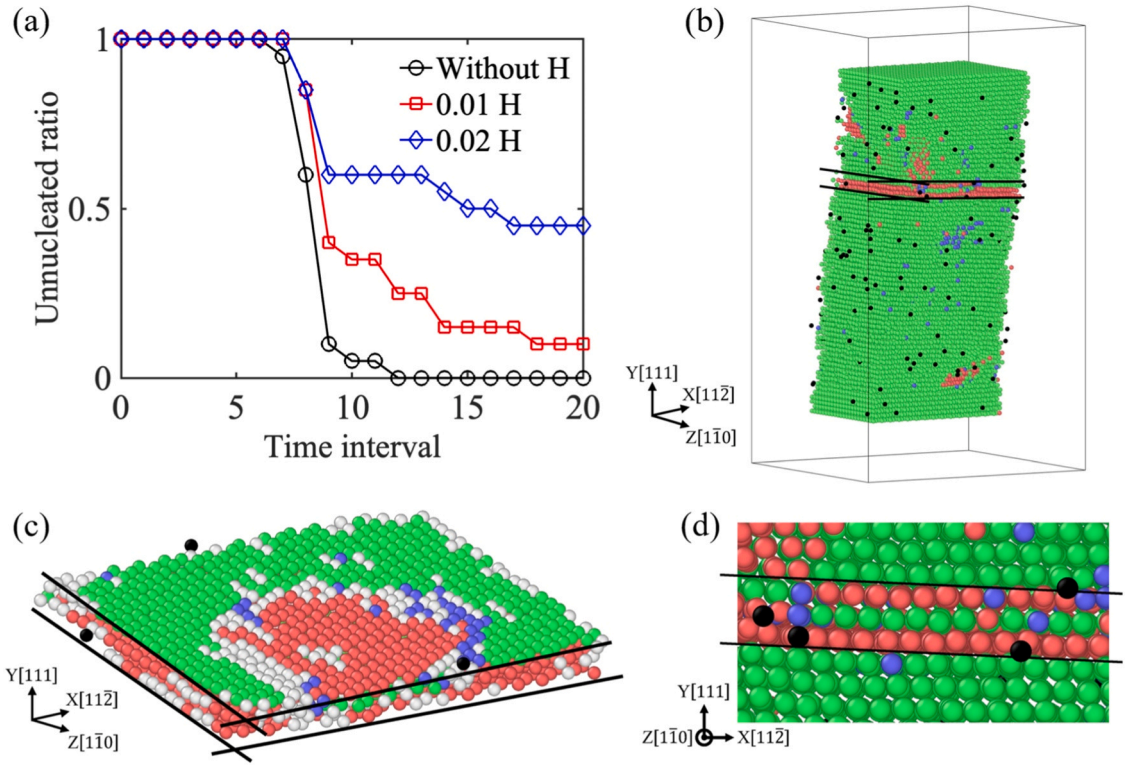

Fig. 3. MD simulation results of twinning nucleation for FeNiCrH systems with free boundaries. (a) Unnucleated twinning ratio $u(k,p)$ versus time interval k for various hydrogen fractions under a shear strain $\gamma_{xy} = 0.047$ and a temperature $T = 750$K. Here the duration time of each interval is $\Delta t = 1$ps. (b) Perspective view of twinning nucleation process in random FeNiCrH system, in which hydrogen atoms are denoted by black spheres. (c) Magnified view of the denoted region in (b), revealing detailed snapshot of surface nucleation process. (d) Magnified side view of the denoted region in (b). In (b)-(d), the Ni atoms located on the surface are removed to display the twin boundaries; the black lines serve as guides to show nanotwinned structure in different views.

behavior observed in homogeneous twinning nucleation, where an accelerated nucleation rate was noted with rising hydrogen fractions. Fig. 3b-d demonstrate that the twinning process with free boundaries is associated with the surface dislocation nucleation process. This observation suggests an assumption that the inhibiting effect of hydrogen is arising from the hydrogen-induced suppression of surface dislocation nucleation. Through in-situ stress relaxation experiments and atomistic simulations in Ag, Yin et al. [30] revealed that the hydrogen located on the surfaces of nanowires would suppress the dislocation nucleation. Our simulation results are aligned with their findings.

4. Twinning nucleation with equilibrium hydrogen atmosphere

In this section, we aim to investigate the role of hydrogen atmosphere in twinning nucleation, considering the hydrogen atoms reach an equilibrium distribution, i.e., hydrogen atoms are situated both within the simulation cell and on its surfaces. We firstly investigate the hydrogen diffusion rate to estimate the relaxation time in the twinning nucleation simulation. For the hydrogen diffusion rate in FeNiCr MEA, we have conducted a series of MD simulations, including 50 samples, to track the trajectory of an individual hydrogen atom at 800 K. In Fig. 4, we present the mean-square displacement of the hydrogen atom as a function of time. Since the hydrogen atom exhibits Brownian motion, its displacement adheres to the classic diffusion equation, i.e., $\langle x^2 \rangle = 2D_{\mathrm{H}}t$, where x is the displacement of the hydrogen atom, D_{H} is the hydrogen diffusion rate and t is the time. Through curve fitting, we can obtain that the hydrogen diffusion rate in FeNiCr MEA is approximately $D_{\mathrm{H}} \approx 1 \times 10^9 \quad \mathrm{m}^2/\mathrm{s}$.

For the MD simulation of twinning nucleation, to ensure consistency, we maintained the same simulation cell and boundary conditions as those employed in Fig. 3. In order to establish the equilibrium

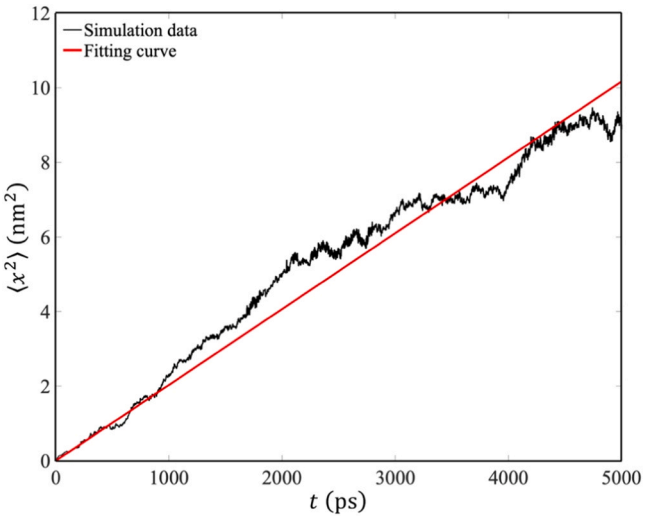

Fig. 4. Mean square displacement of the individual hydrogen atom under 800 K as a function of time. The mean values are obtained by averaging 50 samples with different distributions of Fe, Ni and Cr atoms.

distribution of hydrogen atoms, we initially place hydrogen atoms within the octahedrons inside the simulation cell (as shown in Fig. 5d). Subsequently, we conduct MD simulations in the canonical ensemble (NVT) for a duration of 10ns at a temperature of $T = 800$K. Since the cross section of simulation cell is 7nm × 6nm, the maximum distance of one hydrogen atoms diffusion into the adjacent surface is $\lambda = \frac{7\mathrm{nm}}{2} = 3.5\mathrm{nm}$. Then the rough time estimation of hydrogen diffusion into

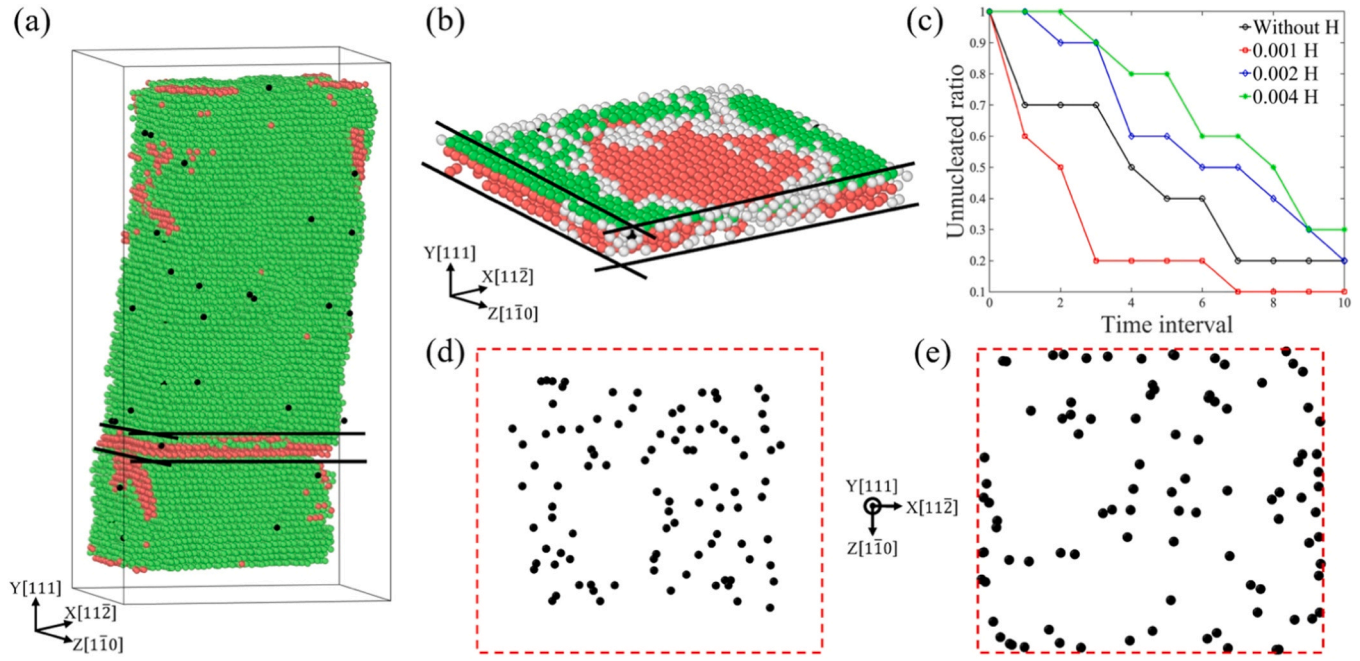

Fig. 5. MD simulation results of twinning nucleation for FeNiCrH systems with equilibrium hydrogen atmosphere. (a) Perspective view of twinning nucleation process in random FeNiCrH system, in which hydrogen atoms are denoted by black spheres. (b) Magnified view of the denoted region in (a), revealing the snapshot of twinning nucleation process. (c) Unnucleated twinning ratio $u(k,p)$ versus time interval k for various hydrogen fractions under a shear strain $\gamma_{xy} = 0.05$ and a temperature $T = 800$K. Here the duration time of each interval is $\Delta t = 1$ps. (d) Top view of the initial hydrogen locations, in which hydrogen atoms are located inside the simulation cell. (e) Top view of relaxed hydrogen locations, in which the hydrogen atoms are both located inside the simulation cell and on the surfaces. In (d) and (e) the red-dashed box roughly represents border of the simulation cell.

adjacent surface is $\frac{\lambda^2}{2D_H} \approx 6$ns, which is less than the time parameter of 10 ns in the MD simulations. Moreover, as the binding energy of hydrogen located on the surface is much lower than that in the octahedrons, there would be an additional force driving the hydrogen atoms to the surface (see Fig. 5e). Then, a canonical ensemble (NVT) was maintained while monitoring the system until twinning occurred. Twinning was induced by applying a resolved shear strain of $\gamma_{xy} = 0.05$ and at a temperature of $T = 800$K.

Fig. 5(a) and (b) reveal that the twining nucleation process is formed by the layer-by-layer surface dislocation nucleation, which is the same as that presented in Fig. 3. As shown in Fig. 5c, the relationship between the unnucleated ratio and the time interval does not follow the theoretically predicted exponential form for any fixed hydrogen number, similar to the case where hydrogen atoms are all located on the surface. This makes it challenging to employ a probability parameter to gauge the level of twinning difficulty. Nevertheless, we can still qualitatively assess the level of twinning nucleation difficulty based on varying hydrogen concentrations. It becomes evident that at low hydrogen fraction ($\chi = 0.001$), the unnucleated ratio is lower than that without hydrogen, suggesting that hydrogen atoms enhance twinning nucleation in that condition. As the hydrogen fraction increases ($\chi = 0.002, 0.004$), the unnucleated ratio rises, indicating that at high hydrogen fraction hydrogen atoms hinder the twinning nucleation process.

A plausible mechanism can be proposed to explain this phenomenon. When the amount of hydrogen is relatively small, only a few hydrogen atoms diffuse onto the surface. In such case, the interior hydrogens primarily influence the twinning nucleation process, leading to the promotion of twinning. However, as the quantity of hydrogen increases, a large number of hydrogen atoms diffuse to the surface. The augmented hydrogen concentration on the surface exerts a more significant impact, which manifests as the inhibitory influence on the twinning process. These observations underscore the intricate interplay between hydrogen and twinning, underscoring the distinct effects stemming from interior hydrogen versus exterior hydrogen.

5. Concluding remarks

In summary, we have conducted a thorough investigation into the impact of hydrogen on twinning nucleation in FeNiCr MEA through atomistic simulations. Our simulations have revealed that the time required for homogeneous twinning nucleation follows the classic Pascal distribution with a success number of $r = 1$. Moreover, our findings indicate that hydrogen atoms facilitate the homogeneous twinning nucleation. In contrast, we have observed that hydrogen atoms located on the surfaces of the alloys exhibit an inhibiting effect on twinning nucleation. This distinction underscores the intricate interplay between hydrogen and twinning mechanisms, highlighting the differing effects arising from interior hydrogen as opposed to exterior hydrogen.

The presence of twin architecture significantly contributes to the alloy's overall strength, ductility and toughness. Consequently, the multifaceted influence of hydrogen atoms on twinning nucleation introduces complexity to the broader scenario of hydrogen's impact on the mechanical properties of MEAs. Through a comprehensive exploration of the hydrogen-twinning relationship, we can attain a profound comprehension of its implications for a material's resistance to hydrogen embrittlement.

This enhanced understanding establishes a fundamental basis for the development of more precise and efficient materials engineered to withstand the challenges posed by hydrogen exposure. Our study not only opens avenues for investigating the hydrogen's effects on twinning nucleation but also sheds light on other deformation mechanisms associated with MEAs. Ultimately, this research contributes to the broader effort of advancing materials science to mitigate hydrogen embrittlement issues and improve the durability of engineering components in hydrogen-rich environments.

CRediT authorship contribution statement

Jinjin Guo: Atomistic simulation, Writing – original draft. **Shuozhi**

Xu: Methodology, Discussion, Writing – review & editing. **Dengke Chen**: Conceptualization, Methodology, Founding acquisition, Writing – review & editing.

Declaration of Competing Interest

The authors declare that they have no known competing financial interests or personal relationships that could have appeared to influence the work reported in this paper.

Data availability

The data for this study can be made available upon reasonable request.

Acknowledgement

The computations in this paper were run on the Siyuan-1 cluster supported by the Center for High Performance Computing at Shanghai Jiao Tong University. D. Chen acknowledges the support from the Shanghai Pujiang Program (21PJ1404800).

References

[1] R.F. Service, The hydrogen backlash, Science 305 (5686) (2004) 958–961, https://doi.org/10.1126/science.305.5686.958.
[2] H.K. Birnbaum, P. Sofronis, Hydrogen-enhanced localized plasticity—a mechanism for hydrogen-related fracture, Mater. Sci. Eng. A. 176 (1–2) (1994) 191–202, https://doi.org/10.1016/S0997-7538(01)01179-2.
[3] S. Bechtle, M. Kumar, B.P. Somerday, M.E. Launey, R.O. Ritchie, Grain-boundary engineering markedly reduces susceptibility to intergranular hydrogen embrittlement in metallic materials, Acta Mater. 57 (2009) 4148–4157, https://doi.org/10.1016/j.actamat.2009.05.012.
[4] J. Song, W.A. Curtin, Atomic mechanism and prediction of hydrogen embrittlement in iron, Nat. Mater. 12 (2013) 145–151, https://doi.org/10.1038/nmat3479.
[5] S. Huang, D. Chen, J. Song, D.L. McDowell, T. Zhu, Hydrogen embrittlement of grain boundaries in nickel: an atomistic study, npj Comput. Mater. 3 (2017) 28, https://doi.org/10.1038/s41524-017-0031-1.
[6] L. Huang L, D. Chen, D. Xie, S. Li, Y. Zhang, T. Zhu, D. Raabe, E. Ma, J. Li, Z. Shan, Quantitative tests revealing hydrogen-enhanced dislocation motion in α-iron, Nat. Mater. 22 (2023) 710–716, https://doi.org/10.1038/s41563-023-01537-w.
[7] J. Guo, Y. Zhang, D. Chen, Hydrogen-induced attractive force between two partials of edge dislocation in nickel, J. Appl. Mech. 90 (7) (2023), 071007, https://doi.org/10.1115/1.4057049.
[8] M.B. Kivy, M.A. Zaeem, Generalized stacking fault energies, ductilities, and twinnabilities of CoCrFeNi-based face-centered cubic high-entropy alloys, Scr. Mater. 139 (2017) 83–86, https://doi.org/10.1016/j.scriptamat.2017.06.014.
[9] Z. Zhang, H. Sheng, Z. Wang, B. Gludovatz, Z. Zhang, E.P. George, Q. Yu, S.X. Mao, R.O. Ritchie, Dislocation mechanisms and 3D twin architectures generate exceptional strength-ductility-toughness combination in CrCoNi medium-entropy alloym, Nat. Commun. 8 (2017) 14390, https://doi.org/10.1038/ncomms14390.
[10] J. Ding, Q. Yu, M. Asta, R.O. Ritchie, Proc. Tunable stacking fault energies by tailoring local chemical order in CrCoNi medium-entropy alloys, Natl. Acad. Sci. U. S. A. 115 (2018) 8919–8924, https://doi.org/10.1073/pnas.1808660115.
[11] X.D. Xu, P. Liu, Z. Tang, A. Hirata, S.X. Song, T.G. Nieh, P.K. Liaw, C.T. Liu, M. W. Chen, Transmission electron microscopy characterization of dislocation structure in a face-centered cubic high-entropy alloy Al0.1CoCrFeNi, Acta Mater. 144 (2018) 107–115, https://doi.org/10.1016/j.actamat.2017.10.050.
[12] E.P. George, D. Raabe, R.O. Ritchie, High-entropy alloys, Nat. Rev. Mater. 4 (2019) 515–534, https://doi.org/10.1038/s41578-019-0121-4.
[13] X. Sun, S. Lu, R. Xie, X. An, W. Li, T. Zhang, C. Liang, X. Ding, Y. Wang, H. Zhang, L. Vitos, Can experiment determine the stacking fault energy of metastable alloys, Mater. Des. 199 (2021), 109396, https://doi.org/10.1016/j.matdes.2020.109396.
[14] A. Vaid, D. Wei, E. Bitzek, S. Nasiri, M. Zaiser, Pinning of extended dislocations in atomically disordered cyrstals, Acta Mater. 236 (2022), 118095, https://doi.org/10.1016/j.actamat.2022.118095.
[15] M. Shih, J. Miao, M. Mills, Stacking fault energy in concentrated alloys, Nat. Commun. 12 (2021) 3590, https://doi.org/10.1038/s41467-021-23860-z.
[16] H. Luo, W. Lu, X. Fang, D. Ponge, Z. Li, D. Raabe, Beating hydrogen with its own weapon: Nano-twin gradients enhance embrittlement resistance of a high-entropy alloy, Mater. Today 21 (10) (2018) 1003–1009, https://doi.org/10.1016/j.mattod.2018.07.015.
[17] H. Luo, Z. Li, W. Lu, D. Ponge, D. Raabe, Corros. Sci. 136 (2018) 403–408.
[18] H. Luo, S.S. Sohn, W. Lu, L. Li, X. Li, C.K. Soundararajan, W. Krieger, Z. Li, D. Raabe, A strong and ductile medium-entropy alloy resists hydrogen embrittlement and corrosion, Nat. Commun. 11 (2020) 3081, https://doi.org/10.1038/s41467-020-16791-8.
[19] C. Wang, K. Han, X. Liu, Y. Zhu, S. Liang, L. Zhao, M. Huang, J. Z. Li, First-principles study of hydrogen-vacancy interactions in CoCrFeMnNi high-entropy alloy, Alloy. Compd. 922 (2022), 166259, https://doi.org/10.1016/j.jallcom.2022.166259.
[20] C.K. Soundararajan, H. Luo, D. Raabe, Z. Li, Hydrogen resistance of a 1 GPa strong equiatomic CoCrNi medium entropy alloy, Corros. Sci. 167 (2020), 108510, https://doi.org/10.1016/j.corsci.2020.108510.
[21] Q. Li, J.W. Mo, S.H. Ma, F.H. Duan, Y.L. Zhao, S.F. Liu, W.H. Liu, S.J. Zhao, C. T. Liu, P.K. Liaw, T. Yang, Defeating hydrogen-induced grain-boundary embrittlement via triggering unusual interfacial segregation in FeCrCoNi-type high-entropy alloys, Acta Mater. 241 (2022), 118410, https://doi.org/10.1016/j.actamat.2022.118410.
[22] H. Luo, Z. Li, D. Raabe, Hydrogen enhances strength and ductility of an equiatomic high-entropy alloy, Sci. Rep. 7 (2017) 9892, https://doi.org/10.1038/s41598-017-10774-4.
[23] A.P. Thompson, H.M. Aktulga, R. Berger, D.S. Bolintineanu, W.M. Brown, P. S. Crozier, P.J. in't Veld, A. Kohlmeyer, S.G. Moore, T.D. Nguyen, R. Shan, M. I. Stevens, J. Tranchida, C. Trott, S.J. Plimpton, LAMMPS - a flexible simulation tool for particle-based materials modeling at the atomic, meso, and continuum scales, Comp. Phy. Comm. 271 (2022) 10817, https://doi.org/10.1016/j.cpc.2021.108171.
[24] X.W. Zhou, C. Nowak, R.S. Skelton, M.E. Foster, J.A. Ronevich, C.S. Marchi, R. B. Sills, An Fe–Ni–Cr–H interatomic potential and predictions of hydrogen-affected stacking fault energies in austenitic stainless steels, Int. J. Hydrog. Energy 47 (1) (2022) 651–665, https://doi.org/10.1016/j.ijhydene.2021.09.261.
[25] A. Stukowski, Visualization and analysis of atomistic simulation data with OVITO–the Open Visualization Tool, Model. Simul. Mater. Sci. Eng. 18 (2010), 015012, https://doi.org/10.1088/0965-0393/18/1/015012.
[26] Y. Fan, Y. Osetsky, S. Yip, B. Yildiz, Onset mechanism of strain-rate-induced flow stress upturn, Phy. Rev. Lett. 109 (13) (2012), 135503, https://doi.org/10.1103/PhysRevLett.109.135503.
[27] Y. Fan, Y. Osetskiy, S. Yip, B. Yildiz, Mapping strain rate dependence of dislocation-defect interactions by atomistic simulations, Proc. Natl. Acad. Sci. U. S. A. 110 (44) (2013) 17756–17761, https://doi.org/10.1073/pnas.1310036110.
[28] Z. Bai, Y. Fan, Abnormal strain rate sensitivity driven by a unit dislocation-obstacle interaction in bcc Fe, Phy. Rev. Lett. 120 (12) (2018), 125504, https://doi.org/10.1103/PhysRevLett.120.125504.
[29] S. Mahajan, G.Y. Chin, Formation of deformation twins in fcc crystals, Acta Met. 21 (10) (1973) 1353–1363, https://doi.org/10.1016/0001-6160(73)90085-0.
[30] S. Yin, G. Cheng, T.H. Chang, G. Richter, Y. Zhu, H. Gao, Hydrogen embrittlement in metallic nanowires, Nat. Commun. 10 (2019) 2004, https://doi.org/10.1038/s41467-019-10035-0.
[31] R.A. Johnson, I. Miller, J.E. Freund, Probability and statistics for engineers, Pearson, 2000.
[32] M. Wen, Z. Li, Thermally activated process of homogeneous dislocation nucleation and hydrogen effects: An atomistic study, Comput. Mater. Sci. 54 (2012) 28–31, https://doi.org/10.1016/j.commatsci.2011.10.034.
[33] X. Zhou, B. Ouyang, W.A. Curtin, J. Song, Atomistic investigation of the influence of hydrogen on dislocation nucleation during nanoindentation in Ni and Pd, Acta Mater. 116 (2016) 364–369, https://doi.org/10.1016/j.actamat.2016.06.061.
[34] Q. Li, H. Sheng, E. Ma, Strengthening in multi-principal element alloys with local-chemical-order roughened dislocation pathways, Nat. Commun. 10 (2019) 3563, https://doi.org/10.1038/s41467-019-11464-7.
[35] X. Li, X. Tang, Y. Guo, H. Li, Y. Fan, Modulating grain boundary-mediated of high-entropy alloys via chemo-mechanical coupling, Acta Mater. 258 (2023), 119228, https://doi.org/10.1016/j.actamat.2023.119228.
[36] Y. Wang, B. Ghaffari, C. Taylor, S. Lekakh, C. Engler-Pinto, L. Godlewski, Y. Huo, M. Li, Y. Fan, Nonmonotonic effect of chemical heterogeneity on interfacial crack growth at high-angle grain boundaries in Fe-Ni-Cr alloys, Phys. Rev. Mater. 7 (2023), 073606, https://doi.org/10.1103/PhysRevMaterials.7.073606.